Global Scientific JOURNALS

GSJ: Volume 7, Issue 9, September 2019, Online: ISSN 2320-9186
www.globalscientificjournal.com

# TECHNO-ECONOMIC SIZING AND OPTIMIZATION OF PV/DIESEL MICROGRID FOR RURAL ELECTRIFICATION.

D. C. Idoniboyeobu[1], S.L. Braide[2] and F. C. Franklin[3]
[1,2&3]*(Department of Electrical Engineering, Rivers State University, Nigeria)*

**ABSTRACT:** *This study considered the stand-alone diesel generator system being operated in remote communities of Niger Delta region of Nigeria; in areas not accessible to grid. It also considered integration of renewable energy system with a view of determining an optimal system design that will be most technically and economically feasible and efficient with considerable environmental impact. A typical location was adopted and renewable energy resource data were verified. PV system was designed and component sizing were performed. Diesel generator, PV-Battery and PV-Diesel hybrid systems were simulated and analysed based on their operational behaviour, technical, economic and environmental constraints. The results showed that PV Battery system has 100% renewable penetration, no emission which made it most environmentally friendlier than other systems but it required a very large battery bank which made it the most expensive system with highest NPC and COE. Diesel generator recorded the highest emission into the environment, with highest fuel consumption. The system cost of this model is relatively higher compared to PV-Diesel hybrid system. However, the PV-Diesel hybrid system had 86.6% PV penetration and showed more benefit of cost saving, emission reduction without compromising reliability over the project life of 25 years.*



***Keywords –*** *Rural electrification, Microgrid, Photovoltaic hybrid,*

## I. INTRODUCTION

Recent research studies shows that more than 1.6 billion people in the world do not have access to electricity and majority of these people are rural dwellers of the developing countries, where the pace of electrification remains slow [1]. Majority of the Nigerian citizens are rural dwellers where there is difficult terrain, no easy access to fuel and electricity grids. Majority of these communities are located at a reasonably long distance from the nearest connection point of a utility grid system. Some of the rural communities are characterized by very low population density, low level of education, and low load density. The push by the federal government of Nigeria to drastically increase the grid capacity to 25,000 MW by 2025, even if the vision is realised, may not favour the extension of the national grid to the coastline communities due to rugged terrains and the privatization of the power sector that is profit driven [2]. Rural electrification forms an integral part of a country's infrastructure, although the infrastructural economic plans for developing countries have not given it sufficiant priority. In various developed and developing countries, rural electrification has been successful in stimulating development. Electricity is one of the primary inputs for economic and social development since its provision is crucial for improving living standards, supporting the development and fostering social activities [3]. Electricity provided to rural communities can increase the quality of life. [4].

In Nigeria, the power supply from the central grid is either not available or very unreliable. Solar energy resources in Nigeria can be harnessed to generate electricity for rural electrification. This can enable communities in remote areas of difficult topographic terrain, where construction of transmission line is not economically viable, have asses to power supply from Renewable Energy Resource (RES). RE has become an important alternative as a power provider in rural systems.[5]. Introduction of RE provides a good opportunity for effective energy decentralization and security to both rural and urban citizens. This could be carried out through distributed generation, solar PV, wind, biomass, and the diesel operated hybrid-microgrid system. A Microgrid system is generally known as the system consisting of small DG stations along with the loads which are capable of going into islanded operation at times of need [6]. Among the many benefits of having a microgrid are that it facilitates DG and high penetration of RES. It also increases power quality and reliability of electric supply. A microgrid having RES will help to reduce burning of fossil fuels and its consequence of global warming. Integration of more than one DG in hybrid systems provides relatively constant electricity at an affordable cost, even when one of the supply systems is shut down.

RES is a veritable source of energy for an islanded system though it is associated with availability constraint. Standalone solar PV or wind energy systems do not produce usable energy for a considerable portion of time during the year. This is due to variable sunshine hours as regards to solar PV, and relatively erratic wind speeds, resulting in underutilization of capacity. The independent use of both solar PV and wind energy results in considerable over-sizing for system reliability. Typical hybrid systems include a conventional generator power by diesel, for example, and a renewable energy source(s) including solar PV, wind or both, and energy storage such as batteries if needed [7]. To achieve an efficient and cost effective autonomous hybrid microgrid system, a proper sizing and optimization of system components are required.

## II. RELATED WORKS

Unit sizing of photovoltaic (PV) panels and wind turbines with energy storage for an islanded microgrid has been studied by many researchers. The criteria for choosing the optimal size of an integrated renewable energy system (IRES) are usually influenced by economic and power reliability factors. There are many methodologies applied to proper unit sizing of an isolated hybrid PV-wind microgrid system. Some of the approach reviews are iterative approach, artificial intelligence, multi-objective design approach, probabilistic approach, analytical approach and computer software design tools [8].

[9] performed a useful investigation of the PV-diesel hybrid system for research and education in Australia. Their focus was on remote areas that are not connected to the grid, and their system comprises a PV module of 1.2 kWp, a 5 kVA diesel generator, a 5 kVA bidirectional inverter and a 13 kWh battery bank. The measurement result showed a performance ratio of 0.6 for the PV-array. The average efficiency of the motor-generator was 1.7 kWh/ltr. The battery efficiency was 0.96 and the system efficiency 0.64. This groundwork study has provided the foundation and information for future studies on optimal control and intelligent control strategies.

## III. METHODOLOGY

This study covered Utu Umuoriji community which is located along the bank of River Niger, South of Ndoni District in Ogba/Egbema/Ndoni LGA of Rivers State, Nigeria. It is located at Latitude $5^{0}26'$ N and Longitude $6^{0}33'$ E. The average daytime temperature of the community ranges from $20^{0}$C to $32^{0}$C throughout the year and its average solar irradiation ranges from 3.6 to 5.4kwh /$m^2$ per day. The community has a verse farmland but the population occupies a portion of about 485,000$m^2$ in a nucleated pattern of settlement. At the time of this assessment the community has 60 households. Their occupations are predominantly peasant farming, hunting, fishing and trading on agricultural produce.
It is a host community of Agip oil and gas exploration Company.
Data required for analyses and investigations include solar irradiation, ambient temperature, and energy demand. The solar irradiation and ambient temperature data were accessed from the NASA database. The electrical load profile data was gathered from an individual household appliance. The method and procedure adopted in this research are described accordingly

### 3.1 Method of Analysis

For a successful sizing and optimization of a microgrid certain considerations were made which followed a proscribed procedure illustrated in figure (3.1).

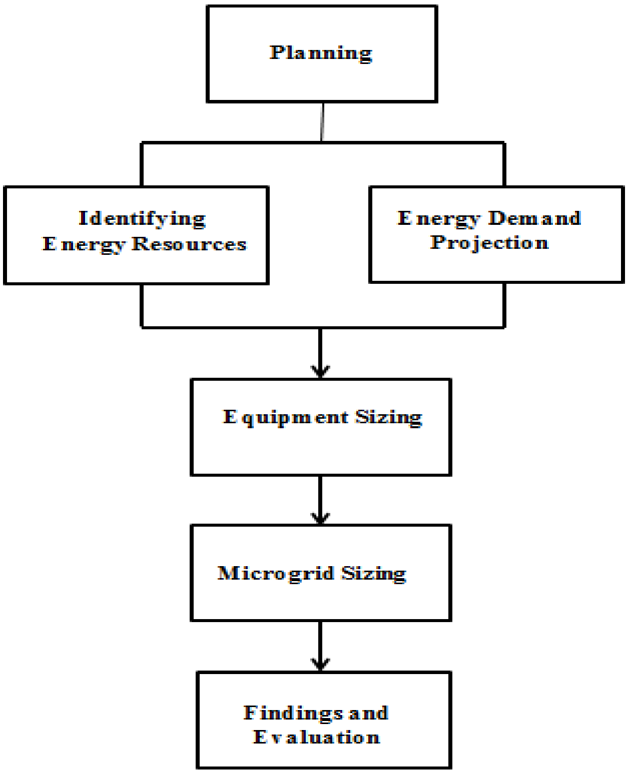


**Figure 3.1 Methodology for Microgrid Design**

#### *3.1.1* Identifying Energy Reserve and Energy Demand Projection

The solar irradiation, ambient temperature data of the Utu-Umuoriji community were accessed from the NASA database and considered to ensure that they are sufficient for adequate power generation. Energy load profile and consumption pattern were constructed with data obtained from electrical appliances in each household and information gathered from members of households.

#### *3.1.2* Equipment Sizing

System component sizing and values were calculated using the deterministic method. Relevant data available from load profile and renewable energy sources were applied in modeled equations arising from theoretical analysis. Relevant component values include PV power rating and required generation capacity, battery bank capacity, converter, and their capacities.

The determined values will be imputed in the simulation software for optimization.

#### *3.1.1* Microgrid Sizing

The Homer simulation tool was used for the optimization of system designs. The values derived from equipment sizing, solar irradiation, ambient temperature, and load profile form input parameters for the simulation software. Different energy system configurations were simulated to determine the optimum hybrid system based on power balance, technical option, cost and specifications to select the optimum scenario according to the isolated community

**Case Study of Design of Off-grid PV-Diesel Hybrid for Utu-Umuoriji Community Electrification**

### 3.2 Identifying Energy Resources

Table: (3.1) shows solar radiation data obtained from NASA's PVGIS database. Once calculated on horizontal area, daily solar irradiation varies from 3.6 kWh/m$^2$/d in July to 5.4 kWh/m$^2$/d in February with an annual average of 4.53 kWh/m$^2$/d.

| Month | Clearness Index | Solar Radiation ($kWh/m^2/day$) |
|---|---|---|
| Jan | 0.6 | 5.4 |
| Feb | 0.5 | 5.4 |
| Mar | 0.7 | 5.2 |
| Apr | 0.5 | 5.0 |
| May | 0.5 | 4.6 |
| Jun | 0.4 | 4.1 |
| Jul | 0.4 | 3.5 |
| Aug | 0.3 | 3.6 |
| Sep | 0.4 | 3.7 |
| Oct | 0.4 | 4.1 |
| Nov | 0.5 | 4.7 |
| Dec | 0.6 | 5.1 |
| **Year Average** | | **4.53** |

**Table 3.1 Solar Irradiation adopted from NASA database Online, accessed on 6/6/2019**

Ambient Temperature is the temperature of the immediate surroundings of the PV module. It has relative effect on the PV cell temperature as shown in Table 3.2 which affects the performance of the PV.

Due to unavailability of measured values of ambient temperature we rely on data obtained from NASA website as shown in Table 3.2. The monthly maximal average temperature is 33.3°C in March when the minimal average temperature is 21.0 °C in September, which makes an annual average of 26.4 °C.

| Month | Average low temperature ($^0C$) | Average low temperature ($^0C$) | Average low temperature ($^0C$) |
|---|---|---|---|
| JAN | 21 | 32 | 26.5 |
| FEB | 23 | 33 | 28.0 |
| MAR | 23 | 33 | 28.0 |
| APR | 23 | 32 | 27.5 |
| MAY | 23 | 31 | 27.0 |
| JUN | 23 | 30 | 26.5 |
| JUL | 22 | 30 | 26.0 |
| AUG | 22 | 29 | 25.5 |
| SEP | 22 | 29 | 25.5 |
| OCT | 22 | 30 | 26.0 |
| NOV | 22 | 31 | 26.5 |
| DEC | 21 | 32 | 26.5 |

**Table 3.2 Ambient Temperature**

### 3.1 Energy Demand Estimation

A design margin ($K_d$) was used to account for any potential inaccuracies in estimating the loads, allow future loads to be supported, system losses and intermittent appliances' startup and shutdown surge

| Hour of Day | Load Power (W) | Load Design Margin + 30% (W) | Design Load Power (W) |
|---|---|---|---|
| 00 | 28,454 | 8,536 | 36,990 |
| 01 | 28,334 | 8,500 | 36,834 |
| 02 | 28,334 | 8,500 | 36,834 |
| 03 | 28,334 | 8,500 | 36,834 |
| 04 | 30,019 | 9,006 | 39,025 |
| 05 | 30,161 | 9,048 | 39,209 |
| 06 | 30,475 | 9,143 | 39,618 |
| 07 | 35,136 | 10,541 | 45,677 |
| 08 | 27,125 | 8,138 | 35,263 |
| 09 | 28,680 | 8,604 | 37,284 |
| 10 | 26,140 | 7,842 | 33,982 |
| 11 | 25,890 | 7,767 | 33,657 |
| 12 | 28,260 | 8,478 | 36,738 |
| 13 | 25,760 | 7,728 | 33,488 |
| 14 | 27,610 | 8,283 | 35,893 |
| 15 | 29,040 | 8,712 | 37,752 |
| 16 | 30,295 | 9,089 | 39,384 |
| 17 | 41,765 | 12,530 | 54,295 |
| 18 | 41,584 | 12,475 | 54,059 |
| 19 | 44,775 | 13,433 | 58,208 |
| 20 | 39,143 | 11,743 | 50,886 |
| 21 | 37,364 | 11,209 | 48,573 |
| 22 | 33,496 | 10,049 | 43,545 |
| 23 | 31,097 | 9,329 | 40,426 |
| Total | 757,271 | | 984,452 |

**Table 3.3 Load profile table**

The peak demand power is 61.12 KW

$$\text{Load factor (L.F)} = \frac{E_d}{P_p * 24hours} \quad (3.1)$$

Where $P_p$ is Peak power

Ed is Energy demand

$$\text{Load factor (L.F)} = \frac{984.7}{61.12 \quad *24hours} = 0.6 \quad (3.2)$$

This section expands the profile load for average daily of every month over a single year hourly consumption profile. The result will be registered in an input file for HOMER simulation tool named as "primary load" parameter.

Based on monthly average residential consumption data, which was gathered from households in Utu-Umuoriji community, an excel sheet was used to develop the village annual consumption load profile.

Table (3.4) shows the hourly average load profile for one day in each month, which is the basic data to further create all the months' hourly energy load values.

| Month | January | February | March | April | May | June | July | August | September | October | November | December |
|---|---|---|---|---|---|---|---|---|---|---|---|---|
| Hour | | | | | | | | | | | | |
| 00 | 38.5 | 35.9 | 38.1 | 38.5 | 35.5 | 35.5 | 35.5 | 37.4 | 37.4 | 36.3 | 36.6 | 38.8 |
| 01 | 38.3 | 35.7 | 37.9 | 38.3 | 35.4 | 35.4 | 35.4 | 37.2 | 37.2 | 36.1 | 36.5 | 38.7 |
| 02 | 38.3 | 35.7 | 37.9 | 38.3 | 35.4 | 35.4 | 35.4 | 37.2 | 37.2 | 36.1 | 36.5 | 38.7 |
| 03 | 38.3 | 35.7 | 37.9 | 38.3 | 35.4 | 35.4 | 35.4 | 37.2 | 37.2 | 36.1 | 36.5 | 38.7 |
| 04 | 40.6 | 37.9 | 40.2 | 40.6 | 37.5 | 37.5 | 37.5 | 39.4 | 39.4 | 38.2 | 38.6 | 41.0 |
| 05 | 40.8 | 38.0 | 40.4 | 40.8 | 37.6 | 37.6 | 37.6 | 39.6 | 39.6 | 38.4 | 38.8 | 41.2 |
| 06 | 41.2 | 38.4 | 40.8 | 41.2 | 38.0 | 38.0 | 38.0 | 40.0 | 40.0 | 38.8 | 39.2 | 41.6 |
| 07 | 47.5 | 44.3 | 47.0 | 47.5 | 43.8 | 43.8 | 43.8 | 46.1 | 46.1 | 44.8 | 45.2 | 48.0 |
| 08 | 36.7 | 34.2 | 36.3 | 36.7 | 33.9 | 33.9 | 33.9 | 35.6 | 35.6 | 34.6 | 34.9 | 37.0 |
| 09 | 38.8 | 36.2 | 38.4 | 38.8 | 35.8 | 35.8 | 35.8 | 37.7 | 37.7 | 36.5 | 36.9 | 39.1 |
| 10 | 35.3 | 33.0 | 35.0 | 35.3 | 32.6 | 32.6 | 32.6 | 34.3 | 34.3 | 33.3 | 33.6 | 35.7 |
| 11 | 35.0 | 32.6 | 34.7 | 35.0 | 32.3 | 32.3 | 32.3 | 34.0 | 34.0 | 33.0 | 33.3 | 35.3 |
| 12 | 38.2 | 35.6 | 37.8 | 38.2 | 35.3 | 35.3 | 35.3 | 37.1 | 37.1 | 36.0 | 36.4 | 38.6 |
| 13 | 34.8 | 32.5 | 34.5 | 34.8 | 32.1 | 32.1 | 32.1 | 33.8 | 33.8 | 32.8 | 33.2 | 35.2 |
| 14 | 37.3 | 34.8 | 37.0 | 37.3 | 34.5 | 34.5 | 34.5 | 36.3 | 36.3 | 35.2 | 35.5 | 37.7 |
| 15 | 39.3 | 36.6 | 38.9 | 39.3 | 36.2 | 36.2 | 36.2 | 38.1 | 38.1 | 37.0 | 37.4 | 39.6 |
| 16 | 41.0 | 38.2 | 40.6 | 41.0 | 37.8 | 37.8 | 37.8 | 39.8 | 39.8 | 38.6 | 39.0 | 41.4 |
| 17 | 56.5 | 52.7 | 55.9 | 56.5 | 52.1 | 52.1 | 52.1 | 54.8 | 54.8 | 53.2 | 53.8 | 57.0 |
| 18 | 56.2 | 52.4 | 55.7 | 56.2 | 51.9 | 51.9 | 51.9 | 54.6 | 54.6 | 53.0 | 53.5 | 56.8 |
| 19 | 60.5 | 56.5 | 60.0 | 60.5 | 55.9 | 55.9 | 55.9 | 58.8 | 58.8 | 57.0 | 57.6 | **61.1** |
| 20 | 52.9 | 49.4 | 52.4 | 52.9 | 48.9 | 48.9 | 48.9 | 51.4 | 51.4 | 49.9 | 50.4 | 53.4 |
| 21 | 50.5 | 47.1 | 50.0 | 50.5 | 46.6 | 46.6 | 46.6 | 49.1 | 49.1 | 47.6 | 48.1 | 51.0 |
| 22 | 45.3 | 42.2 | 44.9 | 45.3 | 41.8 | 41.8 | 41.8 | 44.0 | 44.0 | 42.7 | 43.1 | 45.7 |
| 23 | 42.0 | 39.2 | 41.6 | 42.0 | 38.8 | 38.8 | 38.8 | 40.8 | 40.8 | 39.6 | 40.0 | 42.4 |
| **TOTAL** | **1024** | **955** | **1014** | **1024** | **945** | **945** | **945** | **994** | **994** | **965** | **977** | **1034** |

**Table 3.4 Community Average Load Consumption over 24 Hour**

### 3.2 PV Array Preliminary Sizing

Manual calculation of PV array size will be done in this section which will be used to determine the input values for the simulation and optimization part.

There are three parameters featured in Table (3.5), which are;

i. The Peak Sun Hour (PSH)
ii. The average daily load
iii. The operation ratio

The first two parameters were obtained from (*PVGIS-CMSAF database Online*, *2019*) for the community. The PSH parameter represents the irradiation on the horizontal plane. The average daily load, for each month, is calculated from the consumption data collected from the community households (Table 3.3). The operation ratio is a basic value for sizing a PV system for the "design month" which is the month with highest ratio of load to insulation. The ratio between the average daily load and PSH corresponds to August as the highest ratio, so that the system must be designed to accommodate the energy needs of this month.

| Month | PSH (KWh) | Average daily load (KWh) | Ratio (Average daily load/PSH) |
|---|---|---|---|
| January | 5.4 | 1024 | 190 |
| February | 5.4 | 955 | 177 |
| March | 5.2 | 1014 | 195 |
| April | 5 | 1024 | 205 |
| May | 4.6 | 945 | 205 |
| June | 4.1 | 945 | 231 |
| July | 3.5 | 945 | 270 |
| **August** | **3.6** | **994** | **276** |
| September | 3.7 | 994 | 269 |
| October | 4.1 | 965 | 235 |
| November | 4.7 | 975 | 207 |
| December | 5.1 | 1034 | 203 |

**Table 3.5 Average daily load to PSH ratio table**

To determine the power needed to accommodate the load even at the least PSH, equation (3.3) was applicable.

$$P_{pv} = \frac{E_{LoadTotal}}{PSH.PR} \quad (3.3)$$

$$P_{pv} = \frac{984.7}{3.6*0.75} \quad (3.4)$$

$$P_{pv} = 365\ k \quad (3.5)$$

Where $E_{loadTotal}$ is the total electrical energy load, PSH is the Peak Sun Hour and PR is the performance ratio. The performance ratio estimated value is 75%, the Peak Sun Hours for August is 3.6 kWh and the total electrical load is 984.7 kWh. The power needed is 365 kW.

**2.8 Battery Preliminary Bank sizing**

The size of the batteries is calculated manually using equation (3.10). The result is 1931 kWh assuming that the DoD value is 40%. SF of the battery estimated value is 85% and two DoA is considered. The battery capacity is calculated using a 48V system and the result gives 40,225 Ah.

$$E_{Battery} = \frac{984.7*1}{0.85*(1-{}^{40}/_{100})} \quad (3.6)$$

$$E_{Battery} = 1931\ \text{kWh} \quad (3.7)$$

or

$$\text{Capacity (Ah)} = \frac{1931000}{48} \quad (3.8)$$

$$\text{Capacity (Ah)} = 40{,}225\text{Ah} \quad (3.9)$$

**2.9 Diesel Generator model equation**

The fuel consumption of the diesel generator depends on the rated power of the generator and the actual output power supplied by it. The fuel consumption of the diesel generator ($FC_G$) in (l/h) is given by Equation. (3.9)

$$FC_G = A_G \times P_G + B_G \times P_{R\text{-}G} \quad (3.9)$$

Where $P_G$, $P_{R\text{-}G}$ are the output power and the rated power of the generator in (kW) respectively. $A_G$ and $B_G$ are the coefficients of the consumption curve in (l/kWh).

The fuel consumption of the diesel generator depends on the rated power of the generator and the actual output power supplied by it.

**3.5 System Design and Simulation**

The Hybrid Optimization Model for Electric Renewable (HOMER), is the software developed by the National Renewable Energy Laboratory (NREL). This software simulation tool is used for PV/genset /wind /hydrogen systems design, and economical system size optimization. Three system configurations were simulated with HOMER tool.

I. PV with storage only
II. Diesel generator only

III. PV-Diesel hybrid

The second part is the detailed PV-diesel generator hybrid system component sizing.

3.12**PV Module and Inverter Selection**

Maximum DC power will be generated from PV modules and delivered to the inverter if MPPT device is activated. According to technical data of the SMA SB 5.0 (SMA Sunny Boy PV inverter), the MPPT device will be active if inverter input DC voltage $U_{PV}$ is between 175V and 500V, or:

$U_{MPPT,min}$ =175V≤500V≤$U_{PV}$=$U_{MPPT,max}$

At a given temperature, the voltage range of the PV module can be determined with the equation (3.10)

$$V_{MPPT,T} = V_{MPPT,STC}\left[1 + \frac{T_{K,}P_{MMP}}{100}(T_c - 25)\right] \quad (3.10)$$

Where $T_{K,}P_{MMP}$ is temperature coefficient for voltage changing in MPPT and $V_{MPPT,STC}$ is PV module voltage in Mpp for STC.

For the module type Canadian MaxPower CS6U-340M, the values are given as follows;

$T_{K,}P_{MMP}$ =-0.41%/°C and $V_{MPPT,STC}$ is 37.9V

Considering 15°C as the minimum possible ambient temperature of the location the MPP voltage $V_{MPP}$ is given as;

$$V_{MPPT,15} = 37.9\left[1 + \frac{(-0.41)}{100} * (15 - 25)\right]V \quad (3.11)$$

$$V_{MPPT,15} = 39.45V \quad (3.12)$$

Also, the MPP voltage of the PV module at its maximum operating temperature (85°C) is calculated using equation (3.13)

$$V_{MPPT,85} = 37.9\left[1 + \frac{(-0.41)}{100} * (85 - 25)\right]V \quad (3.13)$$

$$V_{MPPT,85} = 28.57V \quad (3.14)$$

The maximum open circuit voltage can be determined using equation (3.15)

$$V_{OC,T} = V_{OC}\left[1 + \frac{T_{K,}P_{OC}}{100}(T - 25)\right] \quad (3.15)$$

Where $T_{K,}P_{OC}$ is temperature coefficient for voltage changing in open circuit and $V_{OC,STC}$ is PV module voltage in open circuit for STC.

Taking 15°C as the minimum possible ambient temperature of the location then the maximum open circuit voltage ($V_{OC}$) was calculated using equation (3.15)

$T_{K,}P_{OC}$ =-0.31%/°C and $V_{OC,STC}$ is 46.2V

$$V_{OC,15} = 46.2\left[1 + \frac{(-0.31)}{100} * (15 - 25)\right]V \quad (3.16)$$

$$V_{OC,15} = 47.6V \quad (3.17)$$

The maximum short circuit current was calculated at the maximum operating temperature of the PV module (85°C) using equation (3,17)

$$I_{SC,T} = V_{MPPT,STC}\left[1 + \frac{T_{K,}I_{SC}}{100}(T - 25)\right] \quad (3.18)$$

Where $T_{K,}I_{SC}$ is temperature coefficient for current at short circuit and $I_{SC,STC}$ is PV module current at short circuit for STC.

For the module type Canadian MaxPower CS6U-340M, the values are given as follows;

$T_{K,}I_{SC}$ = 0.053%/°C and $I_{SC,STC}$ is 9.48V

$$I_{SC,T} = 9.48\left[1 + \frac{(0.053)}{100} * (85 - 25)\right]A \quad (3.19)$$

$$I_{SC,85} = 9.78A \quad (3.20)$$

Considering the parameters of the inverter and PV module, maximum number of modules per string ($n_{max}$) and minimum number of modules per string ($n_{min}$) was calculated using equations (3.21) and (3.22) respectively.

$$n_{max} = \frac{U_{MPPT,min}}{V_{MPP,85}} \quad (3.21)$$

Where $U_{MPPT,min}$ is minimum input DC voltage of the inverter

$$n_{min} = \frac{175}{28.57}, = 6.1 \quad (3.22)$$

Also,

$n_{max} = \frac{U_{MPPT,max}}{V_{MPP,15}}$ (3.23)

Where, $U_{MPPT,max}$ is maximum input DC voltage of the inverter.

$n_{max} = \frac{500}{39.45}$ = 12.6 (3.24)

$n_{min} \leq n \leq n_{max}$, (3.35)

Where n is the number of modules per string.

Therefore, 7≤11≤12

Maximun string voltage was calculated with equation (3.26)

$V_{OCmax,15} = n * V_{OC,15}$ (3.26)

According to Equation (3.40), for 11 serial connected PV modules input DC voltage to the inverter will be $V_{OC,15}$ =11*47.6 = 523.6V. It is obvious that the input DC voltage to the inverter do not exceed 600V.

Sunny Boy inverter has 2 inputs; input A and input B. The maximum current for each input is 15A while the Maximum short circuit current is 20A.

The $I_{mpp}$ of the PV module is 8.97A while the $I_{sc,85}$ =9.78A. It is obvious that only single string could be permissive in each input making a total of 22 modules. The total PV array rated power is (22*340 = 7,480wp). Practically, the PV array power is designed to be higher than the inverter power since the PV power is based on assumed STC which is never met in reality because other factors such as temperature, efficiency, derating factor reduces the output power by a factor considered as performance ratio described in equation (3.3). This will also ensure that the inverter is not under-utilized to safe cost.

The total PV array power required for the system is 365wp. This will also require 1,074 modules of Canadian MaxPower CS6U-340M and 48 SB5.0 inverters.

| S/N | Canadian MaxPower CS6U-340M | |
|---|---|---|
| 1 | Nominal Power | 340Wp |
| 2 | Optimal Operating Volltage ($V_{mpp}$) | 37.9V |
| 3 | Current ($I_{mpp}$) | 8.97A |
| 4 | Open Circuit Voltage ($V_{oc}$) | 46.2V |
| 5 | Short Circuit Voltage ($I_{SC}$) | 9.48A |
| 6 | Efficiency | 17.49% |
| 7 | Operating Temperature | -40$^0$C - 85$^0$C |
| 8 | Maximum Series Fuse | 15A |
| 9 | Temperature Coefficient of - $P_{mpp}$ ($T_k$, $P_{mpp}$) | -0.41%/$^0$C |
| 10 | Temperature Coefficient of $V_{oc}$ ($T_k$, $V_{oc}$) | -0.31%/$^0$C |
| 11 | Temperature Coefficient of - $I_{SC}$ ($T_k$,$I_{sc}$) | 0.053%/$^0$C |

**Table 3.6 Photovoltaic Module Characteristics**

| S/N | Photovoltaic Inverter Characteristics | | |
|---|---|---|---|
| 1 | Inverter Type | Sunny Boy SB5.0 | |
| 2 | Inverter efficiency | 98% | |
| 3 | Maximum input voltage | 600V | |
| 4 | MPP Voltage range | 175V-500V | |
| 5 | Maximum input current | 15A | |
| 6 | PV inverter size | 5KW | |
| 7 | Lifetime | 15 years | |
| 8 | No of independent MPP input | 2 | |
| 9 | String length | 11 | |
| 10 | String per MPP input A | 11 | |
| 11 | String per MPP input B | 11 | |
| 12 | Total number of modules per 5KW inverter | 22 | |
| | **Inverter details** | **Input A** | **Input B** |
| 13 | Module count | 11 | 11 |
| 14 | Maximum input voltage, $V_{oc}$ at 15°C | 524V | 524V |
| 15 | Minimum input voltage $V_{mpp}$ at 85°C | 313V | 313V |
| 16 | Maximum input current | 15A | 15A |
| 17 | String input current | 9.78A | 9.78A |

**Table 3.7 Photovoltaic Inverter Characteristics**

### 3.14Battery Storage Selection

The battery type selection will affect the designed system lifetime depending on the number of operation cycles. The battery types considered are vented lead-acid, tubular-plate and deep-cycle battery, (Hoppecke 24 OPzS 3000) for this PV system design. The battery specifications are given in Table (3.8). The results shown in this table are from HOMER over PV-diesel hybrid system, the battery loss during charge and discharge is 29,666kWh/year and the storage depletion is 688kWh/year. To protect the battery from overcharging/under charging, charge controller was integrated in the SMA Sunny Island 8.0 bidirectional inverter and it utilizes IUoU charging process.

The battery bank is charged by multiple clusters of sunny Island inverter. Each cluster is made up of 3 Sunny Islands (1 Master and 2 slaves).

Considering a string of 24 batteries, where each battery requires a charging voltage of 2.35V, according to 24 OPzS 3000 datasheet, and string charging voltage is 56.4V. The charging current is limited to $0.6C_{10}$ for fast charging. The value of $C_{10}$ is 3170 and $0.6C_{10}$ is 190.2A.

This design required 10 strings of battery, each string tied to a cluster of 3 Sunny Island and giving at total of 240 batteries, and 30 Sunny Islands. A multicluster box-36 could be installed for control and changing-over in the microgrid. It could be connected to a maximum of 12 clusters. Therefore, the System has 2 clusters spaces for future expansion.

| S/N | Battery Characteristics | |
|---|---|---|
| 1 | Battery type | Hoppecke 24 OPzS 3000 |
| 2 | No of battery in a string | 24 |
| 3 | Battery voltage | 48V |
| 4 | Battery rating | 3000Ah |
| 5 | Battery loss during charging and discharging | 29,666kWh/yr |
| 6 | Storage depletion | 688 kWh/yr |
| 7 | Cost of each battery | $1,100 |
| 8 | Autonomy | 1 days |
| 9 | Dept. of discharge | 40% |
| 10 | Charging voltage | 2.35V |
| 11 | Battery usable energy | 1,029 kWh/day |

**Table 3.8 Battery Characteristics**

### 3.15Multicluster Boxes-32 for Microgrid PCC

This is a point of common coupling (PCC) of stand-alone and hybrid systems connection box. Based on proven technology, 2 to 12 three-phase clusters, each consisting of 3 Sunny Island inverters, can be connected in parallel. To simplify installation, all Multicluster Boxes are completely wired and fitted at the factory and have a main connector for generators, the load distribution and PV or wind turbine systems. All data cables required for the installation are included in the delivery.



## IV. RESULTS AND DISCUSION

### 4.1 Analysis Results

Figure 4.1 illustrates the solar irradiation and clearness index which formed input data for Homer simulation tool. The irradiation data is based on Long-term meteorological data of the location. Precisely the montyly average values of period spanning 22 years, from July 1985 – June 2005, as adapted from NASA surface meteorological and solar database. The annual irradiation data shows that more sunshine was experienced from November to April. These are periods of hamattan and dry season in south-south region. From the month of May, rainfall gradually increases through August and September. In these periods, the region experiences lesser solar sunshine.

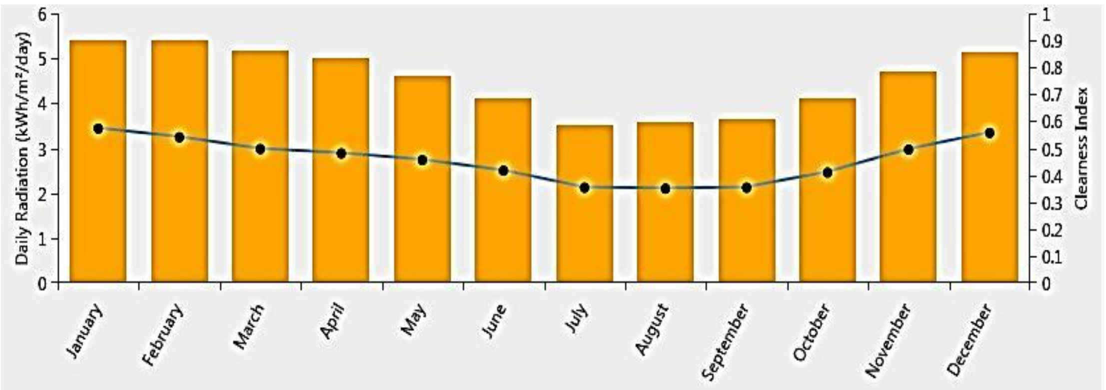


**Figure 4.1 Illustration of solar irradiation**

Electrical energy consumption pattern of the community was illustrated with figure 4.2 and Figure 4.3. More appliances are put to use between the hours of 19:00 and 22:00 when members of various households are back to the house and more activities are carried out at home. The consumption is relatively stable from 23:00 to 04:00 when most people are asleep only essential appliances such as security lightings refrigerators or fans may be ON.

From 05:00 activities resume as members of households get ready for work or school, then it slides down slightly from 08:00. This consumption pattern indicates the characteristics of a typical residential load.

Figure 4.4, illustrates the community's average monthly consumption pattern. Energy consumptions are highest in the months of December and January when member of families abroad come home for Christmas and New Year celebrations. Member of families also return to the community in March/April, this is usually a period of Easter celebration, also various community and family meetings hold at that time. This results to high electric energy demand. The month of August and September also show high demand because schools are on holiday and the children are at home.

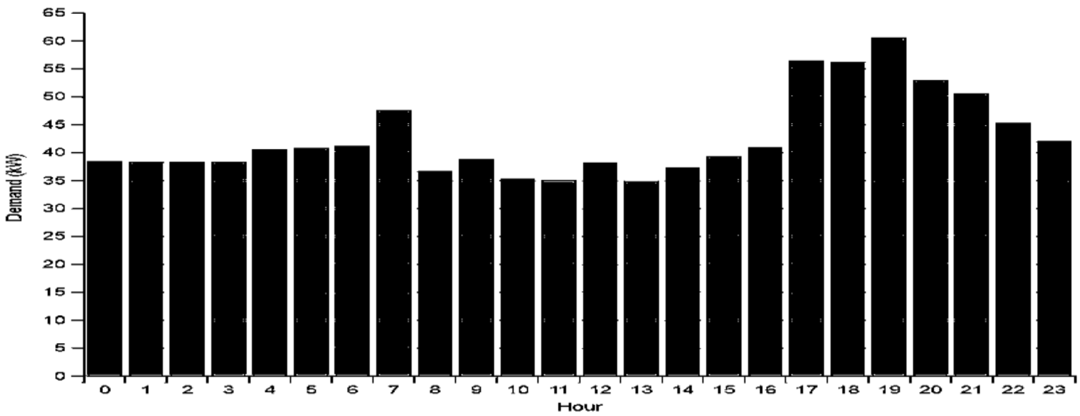


**Figure 4.2 Daily consumption pattern of the community**

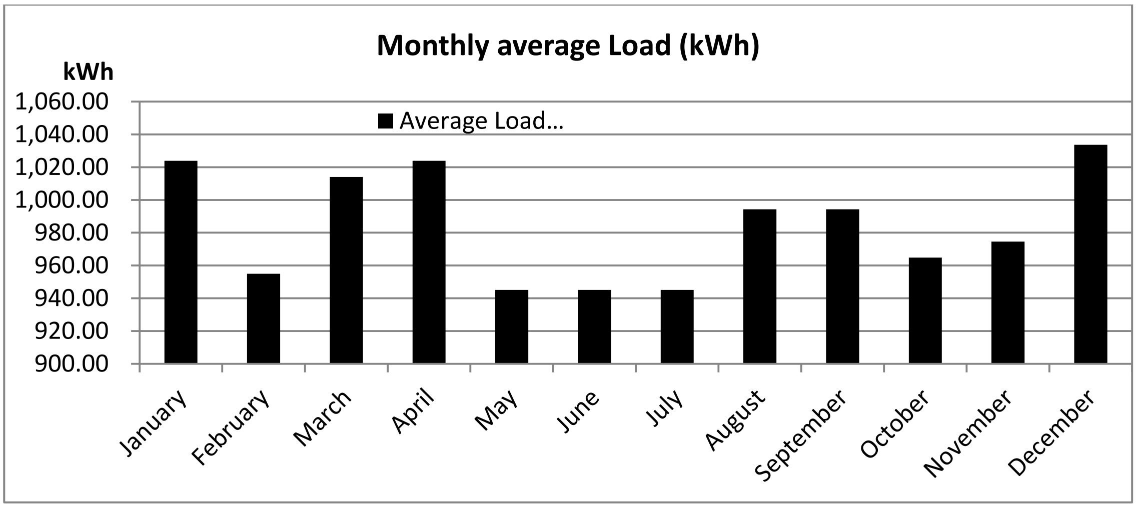


**Figure 4.3 Monthly consumption pattern of the community**

This is an analysis result of three system models. This analysis will cover the technical and economic system performance and environmental effect for 25 years lifetime. The simulation performed with HOMER is aimed towards finding the optimized system based on the cost and size for the existing components.

**Diesel Generator system**

This configuration presents the basic system that supplies the electricity demand of the community. Diesel consumption was 110,836ltr/year.

Figure (4.1) shows the total net present cost (NPC) for the system, which is 2,110,000 USD and the cost of energy (COE) is 0.454 USD/kWh.

| RESULTS | | | | | | | | | | |
|---|---|---|---|---|---|---|---|---|---|---|
| | COE (US$) | NPC (US$) | Operating cost (US$) | Initial capital (US$) | Fuel cost (US$) | O&M (US$) | Ren Frac (%) | Total Fuel (L) | Elec Prod (kWh/yr) | $CO_2$ (kg/yr) |
| | US$0.454 | US$2.11M | US$158,831 | US$54,400 | US$110,836 | US$17,870 | 0 | 110,836 | 359,414 | 290,125 |

**Figure 4.4 Optimized result for Diesel Generator System**

**PV-Battery System**

This system configuration included PV and battery. This model was simulated to examine the advantages and disadvantages of considering 100% renewable energy system. The simulation result is shown in figure 4.6.

RESULTS

| | | | CS6U-340M (kW) | H3000 | Converter (kW) | COE (US$) | NPC (US$) | Operating cost (US$) | Initial capital (US$) | O&M (US$) | Ren Frac (%) | Elec Prod (kWh/yr) | $CO_2$ (kg/yr) |
|---|---|---|---|---|---|---|---|---|---|---|---|---|---|
| | | | 365 | 4,104 | 306 | US$1.25 | US$5.82M | US$53,430 | US$5.13M | US$0.00 | 100 | 474,083 | 0 |

**Figure 4.5 Optimized PV-Battery System.**

PV capacity was 365 kW, 171 strings of battery which consist of 4,104 batteries and provided 29,341 kWh of electricity. The total net present cost (NPC) for the system, which is 5,820,000 USD and the cost of energy (COE) is 1.25 USD/kWh.

**PV-Diesel Hybrid System**

This system configuration was to examine an optimum system with best technical and economic benefit. The result of the simulation was shown in figure 4.7.

RESULTS

| | | | | CS6U-340M (kW) | H3000 | Converter (kW) | COE (US$) | NPC (US$) | Operating cost (US$) | Initial capital (US$) | O&M (US$) | Ren Frac (%) | Total Fuel (L) | Elec Prod (kWh/yr) | $CO_2$ (kg/yr) |
|---|---|---|---|---|---|---|---|---|---|---|---|---|---|---|---|
| | | | | 365 | 240 | 105 | US$0.274 | US$1.27M | US$34,118 | US$832,676 | US$3,036 | 86.6 | 15,563 | 435,919 | 40,738 |

**Figure 4.6 Optimized result for PV-Diesel Hybrid system**

The optimum selection of PV, Diesel generator and batteries provided COE and NPC of 0.374 and 1.27 respectively. The total system cost for the period of 25years which included capital, replacement, M&O, Fuel and salvage was $1,273,733.59. It recorded a renewable percentage of 86.6%and an excess energy of 3.42%.

It is obvious that this system is resented a distinguished cost benefit compared to the other two models described. It could be seen that the lower cost benefit was as a result of lower battery and diesel consumption.

The simulation performed with HOMER in this case includes the PV system and the diesel generator. The operation and maintenance cost is 0.87 USD/h.

**Environmental Analysis**

| | Emission (Kg/year) | | | | | |
|---|---|---|---|---|---|---|
| System Description | Carbon Dioxide | Carbon Monoxide | Unburned Hydrocarbons | Particulate Matter | Sulfur Dioxide | Nitrogen Oxides |
| PV-Battery | 0 | 0 | 0 | 0 | 0 | 0 |
| Diesel Generator Only | 290,125 | 1,829 | 80 | 11 | 710 | 1,718 |
| PV-Diesel Hybrid | 40,738 | 257 | 11 | 2 | 100 | 241 |

**Table 4.1 Emissions**

**Techno-Economic Analysis**

The results obtained showed that the Diesel generator system has no renewable penetration and recorded the highest fuel and maintenance cost making the system economically viable. The PV-Battery system showed the highest PV penetration of 100%, no emission but had the highest NPC and COE of 5,820,000 USD and 1.25 USD/kWh respectively. The high NPC is as a result very large battery bank required. The battery bank size is 4,101 batteries. It also had the highest excess energy. This system is not the best in terms of economic consideration.

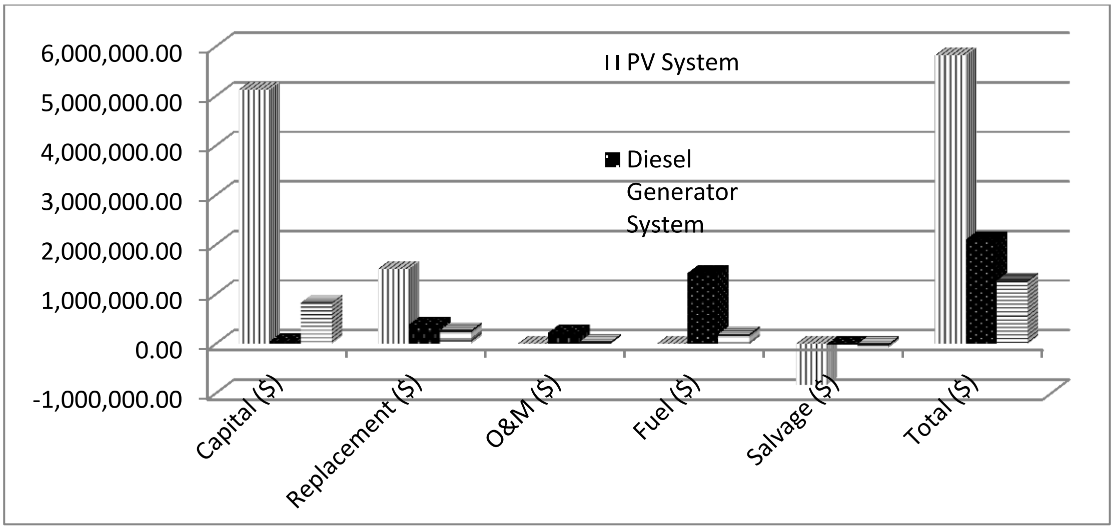


**Figure 4.7 System cost comparison**

## V. CONCLUSION

The performances of three system configurations were examined for a project life of25 years. The results showed that PV Battery system has 100% renewable penetration, no emission which made it most environmentally friendlier than other systems but it required a very large battery bank which made it the most expensive system with highest NPC and COE. Diesel generator recorded the highest emission into the environment and increase greenhouse effect and global warming. It is also identified with highest fuel consumption. The first two systems earlier described are relatively higher in cost compared to PV-Diesel hybrid system. However, the PV-Diesel hybrid system had 86.6% PV penetration and showed more benefit of cost saving, emission reduction of about without compromising reliability.

Future work will be to perform sensitivity simulation and analysis of PV-Diesel hybrid system to further examine the techno-economic characteristics of the system with respect change in system constraints such as load growth, change in prices of PV panel, battery bank and diesel.

**REFRENCES**

[1]. Barnes, D. F., (2012). The Challenge of Rural Electrification: Strategies for Developing Countries. New York: Routledge.

[2]. Diemuodeke, E. O., Addob, A., Dabipi-Kalioa, I., Oko, C. O. C. & Mulugettac, Y. (2017). Energy and Policy Research, 4 (1), 1–9.

[3]. United Nations, 2005

[4]. Kanagawa M. Nataka T. (2008). Assessment of access to electricity and the socio-economic impact in rural areas of developing countries. Energy. Policy,36(6): 2016-2029.

[5]. Hafez, O. & Bhattacharya, K., (2012). Optimal Planning And Design of A Renewable Energy Based Supply System For Microgrids. Renewable Energy, (45), 7–15.

[6]. (IEEE Standards Coordinating Committee, 2011)

[7]. Deshmukh, M. & Deshmukh, S., (2008). Modeling of Hybrid Renewable Energy Systems. Renewable and Sustainable Energy Reviews 12 (1), 235–249.

[8]. Chauhan A. and Saini R., (2014). A review on Integrated Renewable Energy System based power generation for stand-alone applications: Configurations, storage options, sizing methodologies and control, Renewable and Sustainable Energy Reviews, vol. 38, 99-120.

[9]. Che Fung, C., Buntoon, W. & Chern, V. N., 2002. An investigation on the characteristics and performance of a PV-diesel hybrid energy system for teaching and research. 2002 IEEE Region 10 Conference on Computers, Communications, Control and Power Engineering TENCON '02. Proceedings, Volym 3, pp. 1962 - 1965 .